

Limitations and tradeoff in synchronization of large-scale stochastic networks

Amit Diwadkar Umesh Vaidya

Abstract

We study synchronization in scalar nonlinear systems connected over a linear network with stochastic uncertainty in their interactions. We provide a sufficient condition for the synchronization of such network systems expressed in terms of the parameters of the nonlinear scalar dynamics, the second and largest eigenvalues of the mean interconnection Laplacian, and the variance of the stochastic uncertainty. The sufficient condition is independent of network size thereby making it attractive for verification of synchronization in a large size network. The main contribution of this paper is to provide analytical characterization for the interplay of roles played by the internal dynamics of the nonlinear system, network topology, and uncertainty statistics in network synchronization. We show there exist important tradeoffs between these various network parameters necessary to achieve synchronization. We show for nearest neighbor networks with stochastic uncertainty in interactions there exists an optimal number of neighbors with maximum margin for synchronization. This proves in the presence of interaction uncertainty, too many connections among network components is just as harmful for synchronization as the lack of connection. We provide an analytical formula for the optimal gain required to achieve maximum synchronization margin thereby allowing us to compare various complex network topology for their synchronization property.

Index Terms

Mean Square Synchronization, Stochastic Systems, Nonlinear Dynamics

Synchronization in large-scale network systems is a fascinating problem that has attracted researcher attention from various disciplines of science and engineering. Synchronization is a

A. Diwadkar is a Post Doctoral Associate with the Department of Electrical and Computer Engineering, Iowa State University, Ames, IA, 50011 diwadkar@iastate.edu

U. Vaidya is with the Department of Electrical and Computer Engineering, Iowa State University, Ames, IA, 50011 ugvaidya@iastate.edu

ubiquitous phenomena in many engineering and naturally occurring systems. Examples include generators in electric power grids, communication networks, sensor networks, circadian clock, neural network in the visual cortex, biological applications, and synchronization of fireflies [1]–[4]. Synchronization of systems over a network is becoming of significant importance in power system dynamics. Simplified power system models showing synchronization are being studied to gain insight into the effect of network topology on synchronization properties of dynamic power networks [5]. Effect of network topology and size on synchronization ability of complex networks is an important area of research [6]. Complex networks with certain desired properties like small average path between nodes, low clustering ability, existence of hub nodes among others, have been extensively studied over the past decade [7]–[10]. Understanding the effect of neighboring and long range communications on the ability and rate of synchronization, are important questions that will help understand molecular conformation [11]. Emergence of chimera states in synchronization is studied, where for mechanical systems coexistence of asynchronous states with synchronous states is demonstrated [12]. An aspect of network synchronization gaining attention is the effect of network topology and interconnection weights on robustness of synchronization properties [13].

Uncertainty is also ubiquitous in many of these large-scale network systems. Hence, the problem of synchronization in the presence of uncertainty is important for the design of robust network systems. The presence of uncertainty in network systems can be motivated in various different ways. For example, in electric power networks uncertain parameters or outage of transmission lines could be sources of uncertainty. Similarly, a malicious attack on network links can be modeled as uncertainty. Synchronization with limited information or intermittent communication among individual agents, such as a network of neurons, can also be modeled with a time varying uncertainty. In this paper, we address the problem of robust synchronization in large-scale stochastic networks. Existing literature on this problem has focused on the use of Lyapunov function-based techniques to provide conditions for robust synchronization [14]. Similarly problem of synchronization in the presence of simple on-off or blinking interaction uncertainty is studied [15]–[18]. Local synchronization for coupled maps is studied in [19], [20], which provides a measure for local synchronization. Synchronization over balanced neuron networks with random synaptic interconnections is studied [21]. The authors study the emergence of robust synchronized activity in networks with random interconnection weights [22]. Robustness

of synchronization to small perturbations in system dynamics and noise has been studied [23], while robustness to parameter variations is also studied in the context of neuronal behavior [24].

We consider a network of systems where the nodes in the network are dynamic agents with scalar nonlinear dynamics. These agents are assumed to interact linearly with other agents or nodes through the network Laplacian. The interaction among the network nodes is assumed stochastic. This research builds on our past work, where we have developed an analytical framework to understand fundamental limitations for stabilization and estimation of nonlinear systems over uncertain channels [25]–[28]. There are two main motivations for this research, which also form the main contributions of this paper. The first motivation is to provide a scalable computational condition for the synchronization of large-scale network systems. We exploit the identical nature of network agent dynamics to provide a sufficient condition for synchronization, which involves verifying a *scalar* inequality. This makes our condition for synchronization independent of network size; hence attractive from the computational point-of-view for large-scale network systems. The second motivation and contribution of this paper is to understand the *interplay* for the role played by three network parameters, i.e., internal agent dynamics, network topology captured by graph Laplacian, and uncertainty statistics in network synchronization. We provide an analytical expression for the synchronization margin involving all three network parameters that help understand the *tradeoff* between these parameters required for network synchronization. This analytical relationship will provide useful insight and comparison of robustness properties for nearest neighbor networks, with varying number of neighbors. In particular, we show that for a nearest neighbor network there exists optimal numbers of neighbors with a maximum synchronization margin. If the number of neighbors is above or below this optimal value, then the margin for synchronization decreases. We use analytical expression for optimal gain and synchronization margin to compare Small World and Erdos-Renyi network topology for their synchronization property.

I. SYNCHRONIZATION IN NETWORKS WITH UNCERTAIN LINKS

We consider the problem of synchronization in large-scale nonlinear network systems where the scalar dynamics of the individual subsystem is assumed to be of the form

$$x_{t+1}^k = ax_t^k - \phi(x_t^k) + v_t^k \quad k = 1, \dots, N, \quad (1)$$

where, $x^k \in \mathbb{R}$ are the states of the k^{th} subsystem, and $a > 0$ and $v^k \in \mathbb{R}$ is an independent identically distributed (i.i.d.) additive noise process with zero mean (i.e., $E[v_t^k] = 0$) and variance $E[(v_t^k)^2] = \omega^2$. The function $\phi: \mathbb{R} \rightarrow \mathbb{R}$ is a nonlinear function that satisfies the following assumption.

Assumption 1: Nonlinearity $\phi: \mathbb{R} \rightarrow \mathbb{R}$ is a monotonic, globally Lipschitz function with $\phi(0) = 0$, such that,

$$\frac{2}{\delta} (z_1 - z_2) > (\phi(z_1) - \phi(z_2)), \quad \forall z_1, z_2 \in \mathbb{R}.$$

The individual subsystem model is general enough to include systems with steady state dynamics that could be stable, oscillatory, or chaotic in nature. We assume the individual subsystems are linearly coupled over an undirected network given by a graph, $G = (V, E)$, with node set V and edge set E with edge weights $\mu_{ij} \in \mathbb{R}^+$ for $i, j \in V$ and $e_{ij} \in E$. Let $E_U \subseteq E$ be a set of uncertain edges and $E_D = E \setminus E_U$ is the set with deterministic edges. The weights for $e_{ij} \in E_U$ are random variables, $\zeta_{ij} = \mu_{ij} + \xi_{ij}$, where μ_{ij} models the nominal edge weight and ξ_{ij} models the zero mean uncertainty, $E[\xi_{ij}] = 0$, with variance $E[\xi_{ij}^2] = E[(\zeta_{ij} - \mu_{ij})^2] = \sigma_{ij}^2$.

Remark 2: The case corresponding to packet-drop or blinking [16] interaction uncertainty will be a special case of the above defined more general random variable. For example, if $e_{ij} \in E_U$ is a blinking (ON-OFF) interconnection, its weight ζ_{ij} is modeled as a Bernoulli random variable with probability $p < 1$ to be ON and $(1 - p)$ to be OFF. Then corresponding to e_{ij} , we have $\mu_{ij} = p$ and $\sigma_{ij}^2 = p(1 - p)$.

If the coupling gain is $g > 0$ the individual agent dynamics of the coupled subsystem is given by,

$$\begin{aligned} x_{t+1}^k = & a x_t^k - \phi(x_t^k) + g \sum_{e_{kj} \in E_D} \mu_{kj} (x_t^j - x_t^k) \\ & + g \sum_{e_{ki} \in E_U} (\mu_{ki} + \xi_{ki}) (x_t^i - x_t^k) + v_t^k. \end{aligned}$$

As the network is undirected the Laplacian for the network graph is symmetric in nature. We denote the deterministic mean graph Laplacian by $\mathcal{L}_M := [\mu_{ij}] \in \mathbb{R}^{N \times N}$, $e_{ij} \in E$ and zero mean uncertain graph Laplacian by $\mathcal{L}_R := [\xi_{ij}] \in \mathbb{R}^{N \times N}$, $e_{ij} \in E_U$. The mean graph Laplacian may be written as, $\mathcal{L}_M = \mathcal{L}_D + \mathcal{L}_U$ where, \mathcal{L}_D , is the Laplacian for graph over V with edge set E_D ,

and \mathcal{L}_U , is the mean Laplacian for graph over V with edge set E_U . We combine the individual systems to create the network system (\tilde{x}_t) written as,

$$\tilde{x}_{t+1} = (aI_N - g(\mathcal{L}_M + \mathcal{L}_R)) \tilde{x}_t - \tilde{\phi}(\tilde{x}_t) + \tilde{v}_t, \quad (2)$$

where I_N is the $N \times N$ identity matrix, and $\tilde{x}_t = [(x_t^1)' \dots (x_t^N)']'$ and $\tilde{\phi}(\tilde{x}_t) = [(\phi^1)'(x_t^1) \dots (\phi^N)'(x_t^N)]'$. Our objective is to understand the interplay of various network parameters which are the internal dynamics of the network components captured by parameter, a , and nonlinearity, ϕ , the deterministic and uncertain graph Laplacian, $\mathcal{L}_D, \mathcal{L}_U$, the uncertainty characteristics given by the variance, σ_{ij} , of the random variables, and the coupling gain, g for network synchronization. There are four components in Eq. (2) who we expect will play an important role in synchronization. These are the internal dynamics of the network components captured by parameter, a , and nonlinearity, ϕ , the deterministic graph Laplacian, \mathcal{L}_M , the uncertainty characteristics given by the variance, σ_{ij} , of the random variables, and the coupling gain, g . Our objective is to understand the interplay of these components to achieve synchronization in the network.

In the presence of both the multiplicative (i.e., ξ_{ij}) and additive (i.e., v^k) noise processes in the synchronization problem, we propose the following definition of mean square synchronization [29].

Definition 3 (Mean Square Synchronization): The network system (2) is said to be mean square synchronizing, if there exist positive constants, $\beta < 1$, $K(\tilde{e}_0) < \infty$ and $L < \infty$, such that,

$$E_{\Xi} \| x_t^k - x_t^j \|^2 \leq \bar{K}(\tilde{e}_0) \beta^t \| x_0^k - x_0^j \|^2 + L\omega^2, \quad (3)$$

$\forall k, j \in [1, N]$, where \tilde{e}_0 is a function of difference $\| x_0^i - x_0^\ell \|^2$ for $i, \ell \in [1, N]$ and $\bar{K}(0) = K$ for some constant K .

Remark 4: In the absence of additive noise, \tilde{v}_t , in system Eq. (2), the term $L\omega^2$ in Eq. (3) vanishes and Definition 3 then reduces to mean square exponential (MSE) synchronization [30].

We introduce the following definition for the coefficient of dispersion to capture the statistics of uncertainty.

Definition 5 (Coefficient of Dispersion (CoD)): Let $\zeta \in \mathbb{R}$ be a random variable with mean $\mu > 0$ and variance $\sigma^2 > 0$. The coefficient of dispersion γ , is defined as $\gamma := \frac{\sigma^2}{\mu}$.

We make the following assumption on the coupling constants and the coefficient of dispersion.

Assumption 6: For all edges (i, j) in the network, the mean weights assigned are positive, i.e., $\mu_{ij} > 0$ for all (i, j) . Furthermore, the coefficient of dispersion, for each link is given by $\gamma_{ij} = \frac{\sigma_{ij}^2}{\mu_{ij}}$, and $\bar{\gamma} = \max_{\xi_{ij}, e_{ij} \in E_U} \gamma_{ij}$. This assumption simply states the network connections are positively enforcing the coupling.

The goal is to synchronize N first order systems over a network with a mean graph Laplacian, \mathcal{L}_M , having eigenvalues, $0 = \lambda_1 < \lambda_2 \leq \dots \leq \lambda_N$, and maximum link uncertainty dispersion coefficient, $\bar{\gamma}$. Henceforth, we shall call λ_2 and λ_N the boundary eigenvalues. The following theorem is the main result of this paper.

Theorem 7: The network system in Eq. (2), satisfying Assumptions 1 and 6 is mean square synchronizing, if there exists a positive constant, p , that satisfies

$$\delta > p > \alpha_0^2 p + \alpha_0^2 \frac{p^2}{\delta - p} + \frac{1}{\delta}, \quad (4)$$

where $\alpha_0^2 = (a_0 - \lambda_{sup}g)^2 + 2\bar{\gamma}\tau\lambda_{sup}g^2$, $a_0 = a - \frac{1}{\delta}$, and $\lambda_{sup} = \underset{\lambda \in \{\lambda_2, \lambda_N\}}{\operatorname{argmax}} \left| \lambda + \bar{\gamma} - \frac{a_0}{g} \right|$. Furthermore, $\tau := \frac{\lambda_{N_U}}{\lambda_{N_U} + \lambda_{2_D}}$, where λ_{N_U} , is the maximum eigenvalue of \mathcal{L}_U , and λ_{2_D} , is the second smallest eigenvalue of \mathcal{L}_D .

The proof is available in the appendix.

The sufficient condition for a mean square synchronization of N dimensional network system (2) as derived in Theorem 7 is provided in terms of a scalar inequality instead of an N dimensional matrix inequality. Hence, the condition is independent of network size, thereby making it attractive from a computational point-of-view for large-scale networks.

It should be noted the sufficient condition as provided in Theorem 7 (i.e., Eq. (4)) is a Riccati equation in one dimension. For the scalar random variable, ζ_c , writing $E[\zeta_c] = \mu_c := \lambda_{sup}$, $E[(\zeta_c - \mu_c)^2] = \sigma_c^2 := 2\bar{\gamma}\tau\lambda_{sup}$, we can write Eq. (4) as

$$p > E_{\xi_c} \left[(a_0 - \xi_c g)^2 p + (a_0 - \xi_c g)^2 \frac{p^2}{\delta - p} + \frac{1}{\delta} \right]. \quad (5)$$

In fact, the above condition is a sufficient condition for stability of the following scale nonlinear system.

$$x_{t+1} = (a - \zeta_c g) x_t - \phi_0(x_t), \quad \frac{2}{\delta} x > \phi_0(x), \quad (6)$$

where ζ_c is an i.i.d. random variable with mean, μ_c , variance, σ_c^2 , and nonlinearity, ϕ_0 , satisfying Assumption 1. The CoD for ζ is given by $\gamma_c = \frac{\sigma_c^2}{\mu_c \tau} = 2\bar{\gamma}$. Condition (5) is obtained by solving the Lyapunov stability condition for (6) with Lyapunov function $V(x_t) := px_t^2$. Rewriting (5) as

$$\left(p - \frac{1}{\delta}\right) \left(\frac{1}{p} - \frac{1}{\delta}\right) > (a_0 - \mu_c g)^2 + \sigma_c^2 g^2. \quad (7)$$

We see if $V(x_t) = px_t^2$ is a valid Lyapunov function, then so is $\tilde{V}(x_t) = \frac{1}{p}x_t^2$. Apart from stability verification, the Lyapunov function also provides information about the margin for synchronization. In particular, for the parameter's values when the inequality (7) is maximal the synchronization margin is maximal and for parameters values when the inequality (7) becomes equality, the network is on the verge of desynchronization. Since $(p - \frac{1}{\delta}) \left(\frac{1}{p} - \frac{1}{\delta}\right) < (1 - \frac{1}{\delta})^2$, we can conclude inequality (7) is maximal when $p = 1$. For the value of $p = p^* = \frac{1}{p^*}$, the inequality becomes an equality with

$$p^* = \frac{\delta}{2} \left(\kappa + \sqrt{\kappa^2 - \frac{4}{\delta^2}} \right), \quad (8)$$

where $\kappa = 1 + \frac{1}{\delta^2} - ((a_0 - \mu_c g)^2 + \sigma_c^2 g^2)$. Using this, we define the margin for synchronization as follows.

Definition 8 (Synchronization Margin): The margin for synchronization for network system (2) is given by

$$\rho_{SM} := \frac{p^* - 1}{\delta} = \frac{1}{2} \sqrt{\kappa - \frac{2}{\delta}} \left(\sqrt{\kappa - \frac{2}{\delta}} + \sqrt{\kappa + \frac{2}{\delta}} \right). \quad (9)$$

This synchronization margin can be interpreted as how far the network is from the verge of desynchronization. The larger the value of ρ_{SM} , the further away the network is from the verge of desynchronization. We now discuss the impact of $\tau = \frac{\lambda_{N_U}}{\lambda_{N_U} + \lambda_{2_D}}$, capturing the effect of location and cardinality of the uncertain links, on the synchronization margin.

Remark 9 (Significance of τ): The factor $\tau := \frac{\lambda_{N_U}}{\lambda_{N_U} + \lambda_{2_D}}$, in Theorem 7 captures the effect of location and number of uncertain links, whereas $\bar{\gamma}$ captures the effect of intensity of the randomness in the links. It is clear that $0 < \tau \leq 1$. If the number of uncertain links ($|E_U|$) is sufficiently large, the graph formed by purely deterministic edge set (E_D), may become

disconnected ($\lambda_{2_D} = 0$), making $\tau = 1$. In contrast, if a single link is uncertain, say $E_U = \{e_{kl}\}$, then $\tau = \frac{2\mu_{kl}}{2\mu_{kl} + \lambda_{2_D}}$. Hence, for a single uncertain link, the weight of the link is proportional to degradation in synchronization margin. Since, $\lambda_{2_D} \leq \lambda_2$, lower algebraic connectivity of the deterministic graph further degrades the synchronization margin. Based upon this observation, we can rank order individual links within a graph, with respect to their degradation of the synchronization margin, on the basis of location (λ_{2_D}), mean connectivity weight (μ), and the intensity of randomness given by CoD γ . The impact of uncertain link capacities and location poses some interesting problems about their role in desynchronization and clustering of network systems, which will be the topic of a future study.

Next, we discuss the significance of the largest eigenvalue of Laplacian as it applies to our synchronization problem.

A. Significance of Laplacian Eigenvalues

The second smallest eigenvalue, $\lambda_2 > 0$, of the graph Laplacian indicates algebraic connectivity of the graph. We observe from Theorem 7, as (4) is a quadratic in λ , there exist critical values of $\lambda_2(\lambda_N)$ for the given system parameters and CoD, below(above) which synchronization is not guaranteed, respectively. Hence, critical λ_2 indicates we require a minimum degree of connectivity within the network to accomplish synchronization. To understand the significance of λ_N , we look at the complement of the graph on the same set of nodes. We know from [31], sum of largest Laplacian eigenvalue of a graph and second smallest Laplacian eigenvalue of its complement is constant. Thus, if λ_N is large then the complementary graph has low algebraic connectivity. If we have hub nodes with high connectivity, then these nodes are sparsely connected in the complementary graph. Hence, high λ_N indicates a high presence of densely connected hub nodes. Therefore we conclude strong robustness property in synchronization is guaranteed for close to average connectivity of nodes as compared to isolated highly connected hub nodes.

II. OPTIMAL NEIGHBORS IN NEAREST NEIGHBOR NETWORKS

The analytical formula for the synchronization margin (9) provides us with a powerful tool to understand the effect of various network parameters on the synchronization margin. In this section, we investigate the effect of the number of neighbors on the synchronization margin.

We consider a nearest neighbor network with $N = 1000$ nodes and increase the number of neighbors to study its impact on the synchronization margin. The other network parameters are set to $a = 1.05$, $\delta = 2$, coupling gain $g = \frac{1}{N}$, and CoD of $\bar{\gamma} = 25$. We choose a large number of uncertain links (70%), such that $\tau \approx 1$ to remove the bias of uncertain link location. We show the plot for the synchronization margin against the number of neighbors in Fig. 1(a). From this plot, we see there is an optimal number of neighbors an agent needs to maximize the margin of synchronization. There is a minimum number of neighbors an agent needs below which the network will not synchronize. However, an uncertain environment with too many neighbors is also detrimental to synchronization. This result highlights the fact, while "good" information is propagated through neighbors via network interconnection, these same neighbors in an uncertain environment can propagate "bad" information detrimental to reaching agreement. In Fig. 1(b), we show the plot for the change in the synchronization margin with a change in the number of neighbors for different values of CoD. We notice for a larger value of CoD, the drop in margin with the increase in network connectivity is more dramatic.

In the light of the previous discussion, we can also interpret the coupling gain, g , as the trust shown by a given agent in the information provided by its neighbors. In particular, if the coupling gain, g , is large, then the agent has more trust on its neighbors. In Fig. 1(c), we show the effect of increasing the coupling gain, g , on the synchronization margin. We observe the higher the trust an agent has in its neighbor, the lower the number of neighbors it needs to achieve synchronization. However, in an uncertain environment, with more trust on its neighbors, an agent needs to avoid making more neighbors, as it is detrimental to synchronization. On the other hand, if it has lower trust in its neighbors, an agent requires forging more connections and gathering as much information as possible, even if it is corrupted. Thus, forging connections is good for a group with a goal of synchronization, but there is a critical number of neighbors beyond when the returns from forging new connections diminishes.

III. INTERPLAY OF INTERNAL DYNAMICS, NETWORK TOPOLOGY, AND UNCERTAINTY CHARACTERISTICS

In this section, we discuss the role played by the internal dynamics, network topology, and uncertainty statistics for the synchronization of the network system. The internal dynamics is captured by parameters a and δ , the network topology is captured by the mean deterministic

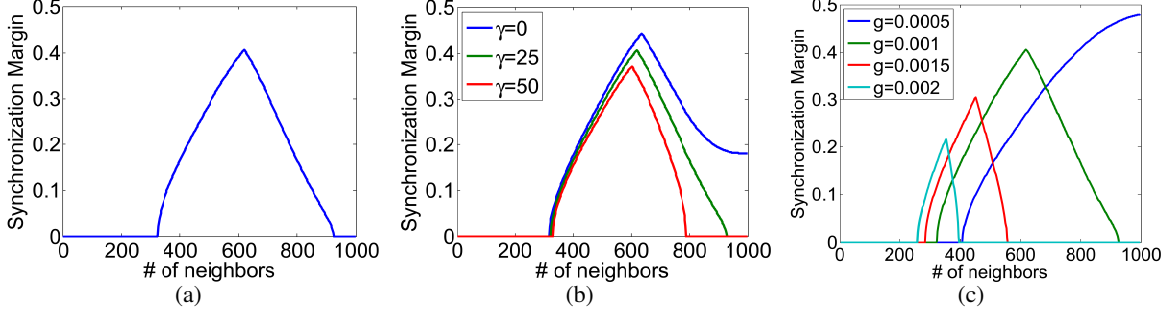


Fig. 1: (a) Synchronization margin for $a = 1.05$, $\delta = 2$, $g = 0.001$ and $\bar{\gamma} = 1$ as the number of neighbors are varied in a nearest neighbor graph, (b) Synchronization margin for $a = 1.05$, $\delta = 2$, and $g = 0.001$ for different $\bar{\gamma}$ as the number of neighbors are varied in a nearest neighbor graph, (c) Synchronization margin for $a = 1.05$, $\delta = 2$, and $\bar{\gamma} = 10$ for different coupling gains as the number of neighbors are varied in a nearest neighbor graph.

Laplacian, \mathcal{L}_M , in particular, the boundary eigenvalues of the Laplacian, and the uncertainty statistics is captured by CoD $\bar{\gamma}$. We will make use of results from Theorem 7 and Definition 8 for the robust synchronization margin to uncover the interplay between the various parameters. Once again, to nullify the bias of uncertain link location, we choose to work with a large number of uncertain links to obtain $\tau \approx 1$.

Consider $\lambda_2 > 0$ and λ_N to be the boundary eigenvalues of the deterministic mean graph Laplacian \mathcal{L}_M . When the fluctuations in link weights are zero (i.e., CoD $\bar{\gamma} = 0$), the critical value of λ_2 below, which synchronization is not guaranteed, is $\lambda_2^* = \frac{a-1}{g}$. Furthermore, synchronization is not guaranteed for λ_N above the critical value, $\lambda_N^* = \frac{a+1}{g} - \frac{2}{g\delta} = \lambda_2^* + \frac{2}{g} \left(1 - \frac{1}{\delta}\right)$. Thus, we see that $\partial\lambda^* := \lambda_N^* - \lambda_2^* = \frac{2}{g} \left(1 - \frac{1}{\delta}\right)$ and $\rho^* := \frac{\lambda_N^*}{\lambda_2^*} = 1 + \frac{2}{a-1} \left(1 - \frac{1}{\delta}\right)$.

In Fig. 2(a), we study the interplay of network topology, uncertainty, and the internal dynamics in the three-dimensional parameter space of $a - \lambda - \bar{\gamma}$. In Fig. 2(a), the region inside (outside) the tunnel corresponds to the combination of parameter values, where synchronization is possible (not possible). We see while the $\partial\lambda^*$ is independent of internal dynamics parameter a , λ_2^* increases with the increase in the value of a . In fact, for $a = 1 + \epsilon$ where $\epsilon > 0$ is arbitrary small, we have $\lambda_2^* = \frac{\epsilon}{g}$. Hence the synchronization can be achieved with a low degree of network connectivity. But, as the internal dynamics become more unstable, we require an increase in the degree of connectivity among network agents to achieve synchronization. The expression for $\partial\lambda^*$ and ρ^* provide insight into the precise tradeoff between the internal dynamics and network topology for $\bar{\gamma} = 0$. Another important observation we make from Fig. 2(a) is the area inside the tunnel

increases with a decrease in internal instability or value of a . This implies with the decrease in parameter value a , there is an increase in feasible region of synchronization in $\lambda - \bar{\gamma}$ space. Now, since $\partial\lambda^*$ does not change with a , the increase in the feasible region is made possible due to an increase in the admissible value of $\bar{\gamma}$.

In Fig. 2(b), we plot the effect of changing nonlinearity bound δ , on the synchronization margin in the $\delta - \lambda - \bar{\gamma}$ space. As δ is increased, the region of synchronization is observed to increase. Thus, a minimally nonlinear system is able to achieve synchronization even with high levels of communication. On the other hand, as the nonlinearity in a system becomes significant, the interaction of the nonlinearity and the fluctuations in the links weights could have adverse effects under a highly connected network. Intuitively, as high communication indicates amplification of uncertainty within agents, one might think of this as the uncertainty in the fluctuations being wrapped around and amplified by the nonlinearity leading to desynchronization under high communication. In Fig. 2(c), we plot a slice of the synchronization regions from both Figs. 2(a) and 2(b), highlighting the synchronization margin.

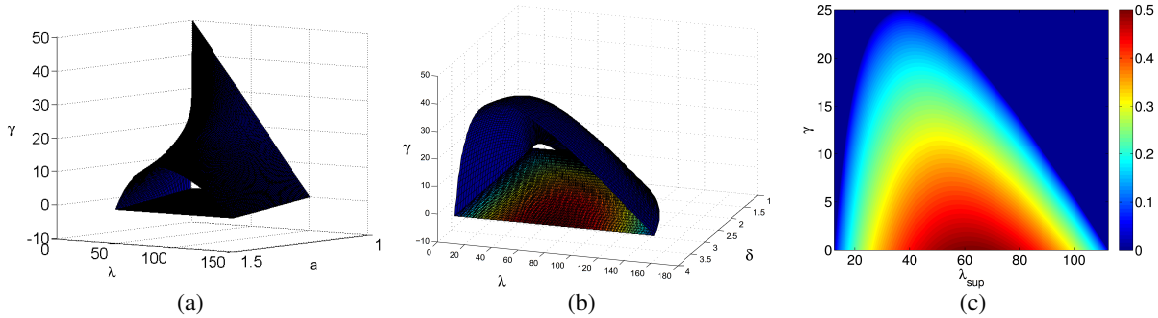


Fig. 2: (a) $a - \lambda - \bar{\gamma}$ parameter space indicating synchronization margin for $g = 0.01$, and $\delta = 2$, (b) $\delta - \lambda - \bar{\gamma}$ parameter space indicating synchronization margin for $a = 1.125$ and $g = 0.01$, (c) $\lambda - \bar{\gamma}$ parameter space indicating synchronization margin for $a = 1.125$, $g = 0.01$, and $\delta = 2$.

We now show how the main results of this paper, in particular, the expression for synchronization margin, can be used to determine optimal value of coupling gain, g^* , to maximize the margin of synchronization for a given network topology (i.e., specific values of λ_2 and λ_N) and uncertainty (i.e., CoD value $\bar{\gamma}$). We assume for given values of λ_2 , λ_N , and $\bar{\gamma}$, there exists value of g for which synchronization is possible. We now state a Lemma that provides a method to find the optimal coupling gain for synchronization over a given network.

Lemma 10: For the network system (2) satisfying Assumptions 1, 6, and condition for synchronization 4, the optimal gain, g^* , to achieve maximum synchronization margin is given by

$$g^* = \frac{2(a - \frac{1}{\delta})}{\max\{\lambda_N, \lambda_2 + 2\bar{\gamma}\tau\} + \lambda_2 + 2\bar{\gamma}\tau}. \quad (10)$$

The proof is available in appendix.

A. Optimal gain for complex networks

Based on Lemma 10 we can now compare performance of some well known random networks topology and the optimal gain required to synchronize systems over these networks. In these simulations the instability of the system is considered to be, $a = 1.05$, the nonlinearity bound, $\delta = 4$, and the uncertainty statistics given by CoD is $\bar{\gamma} = 1$. Furthermore, we choose $\tau \approx 1$. The properties of the random networks are studied for four different network sizes $N \in \{80, 100, 120, 140\}$, N being the number of nodes. In Fig. 3(a) we plot the optimal gain for the Erdos-Renyi (ER) networks as the function of edge connection probability. It is well known that for an Erdos-Renyi network of size N to be connected, the probability of connection must be $p \geq \frac{\log N}{N}$. Hence we plot these networks for probabilities ranging from $p = 0.2$ to $p = 1$. At $p = 1$ we obtain an all to all connection network as each edge is connected with unit probability.

In Fig. 3(d) we plot the corresponding optimal synchronization margin for the ER network. Though the ER networks were one of the first random networks studied, they do not capture real world network properties. To better capture these properties Small World (SW) networks we introduced [8]. In Figs. 3(b), and 3(e), we plot the optimal gain and optimal synchronization margin respectively, for SW networks with varying probability p [8]. To better observe the contrast in behavior of both the ER and SW random networks we plot in Fig. 3(c) the optimal gain for an ER and SW network with $N = 100$ nodes. We notice that while larger gain is required to synchronize the ER network compared to SW network for smaller value of probability, the optimal gain for the ER network decreases over SW network for larger value of p .

In Figs. 3(d),3(e) and 3(f), we plot the optimal synchronization margin for the two networks. We notice that there is bump increase in the synchronization margin for the ER network around $p = 0.5$. From these plots (specifically Figs. 3(c) and 3(f) we draw a conclusion that, for the given set of parameters, ER (SW) network has better synchronization property (i.e., smaller value

of optimal gain and larger margin of synchronization) for larger (smaller) value of probability p . The transition in probability happen between $p = 0.2$ and $p = 0.4$.

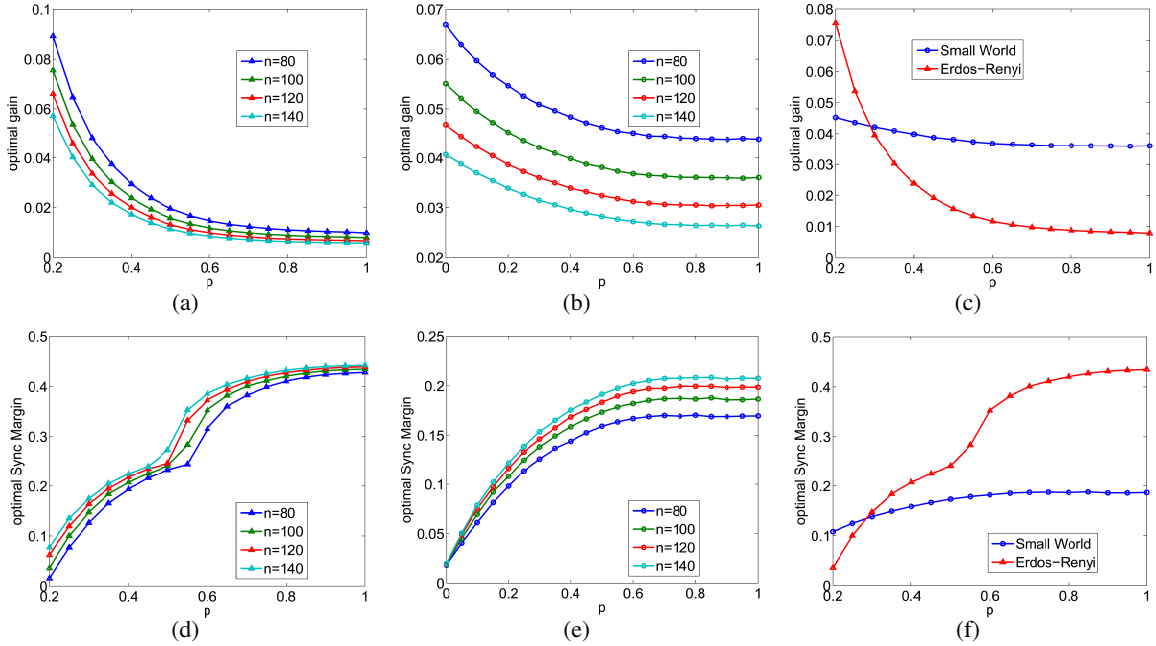


Fig. 3: Optimal gain computation for varying network sizes (a) Erdos-Renyi (ER) networks with probability p of link connection, (b) Small World (SW) networks with rewiring probability p , (c) Optimal gain comparison for ER and SW networks with $n = 100$, Optimal synchronization margin for varying network sizes (d) Erdos-Renyi networks, (e) Small World networks, (f) Optimal synchronization margin comparison for ER and SW networks for $n = 100$.

IV. SIMULATION RESULTS

We consider the following 1D system,

$$x_{t+1} = ax_t - \phi(x_t) + v_t, \quad (11)$$

where $a = 1.125$, $\delta = 8$ and v_t is additive white Gaussian noise with zero mean and variance ω^2 . Here, $\phi(x)$ is given by

$$\phi(x_t) = \frac{\text{sgn}(x_t)}{8} \left(s_1 (|x_t| - \epsilon) + (s_2^2 (|x_t| - \epsilon)^2 + s_3)^{\frac{1}{2}} \right),$$

where $s_1 = 1 + m_2$, $s_2 = 1 - m_2$, $s_3 = 4m_2\epsilon^2$, $m_2 = \frac{1}{1+10\epsilon^{0.1}}$, and $\epsilon = 0.3$. The internal dynamics of the system as described by Eq. (11) consists of double well potential, with an unstable

equilibrium point at the origin and two stable equilibrium points at $x^* = \pm\epsilon \left(\frac{a-1}{a-2} + \frac{m_2(a-1)}{m_2(a-1)-1} \right) = \pm 0.5237$. So, with no network coupling, i.e., $g = 0$, the internal dynamics of the agents will converge to the positive (negative) equilibrium point $x^* > 0$ ($x^* < 0$) for positive (negative) initial conditions. The double well potential system is a prototypical example for modeling synchronization phenomena occurring in natural science and engineering systems. For example, collective motion in molecular dynamics [11] and synchronization of generators in power grid [4] can essentially be modeled using double well potential.

A. Effect of coupling gain

We couple this system over a network of 100 nodes, generated as a random network with the Small World property. The coupling gain for this system is $g = 0.005$. The mean Laplacian of the network is a standard Laplacian with unit weight. Thus, for all links e_{ij} connecting nodes i and j , $\mu_{ij} = 1$. This network has $\lambda_N = 52.55$ and $\lambda_2 = 26.23$. We now choose 60% of the links in the network to have uncertain weights making $\tau \approx 1$. The uncertainty in the network link weights is chosen as a uniform variable with zero mean and variance, $\sigma^2 = 2$ with CoD $\bar{\gamma} = \frac{\sigma^2}{\mu} = 2$, such that both these eigenvalues satisfy the required condition from Theorem 7. The CoD of the link uncertainty is $\bar{\gamma} = \frac{\sigma^2}{\mu} = 2$. In Fig. 4(a), we plot the results for synchronization of these 100 systems with simulated additive white gaussian noise with zero mean and variance $\omega^2 = 0.1$, which shows the systems synchronize in an interval around the equilibrium point.

If the coupling gain is decreased to $g = 0.001$, which does not satisfy the requirement for Theorem 7, we observe the system is not able to synchronize (Fig. 4(b)), and the points with positive initial conditions converge to the positive equilibrium and visa-versa for the points with negative initial conditions. We do see some movement to the opposing equilibrium point for initial conditions very close to the origin. This may be possible due to the connectivity of such nodes to nodes in the other well and the fact they are extremely close to the origin, which creates a dividing barrier between the two potential wells, such that any small computational inaccuracy or stochasticity allows it to overcome the potential barrier.

B. Effect of number of neighbors

Next we study the effect on the group's synchronization ability due to change in the number of neighbors for an agent. For this we choose a nearest neighbor network with 100 nodes. The

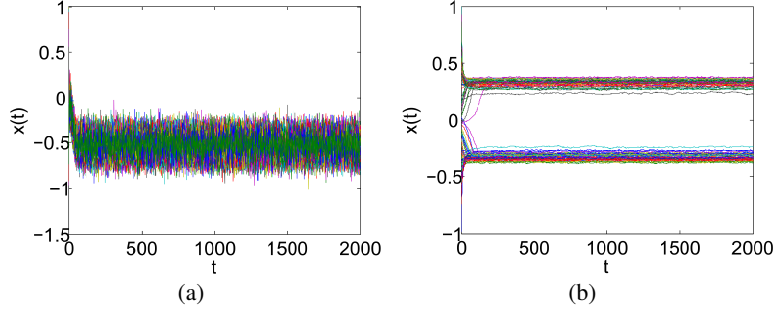


Fig. 4: (a) Time evolution of systems over a 100-node Small World network, $\bar{\gamma} = 2$, $g = 0.01$, (b) Time evolution of systems over a 100-node Small World network, $\bar{\gamma} = 2$, $g = 0.001$.

simulation parameters are chosen as, $a = 1.05$, $\delta = 16$, $g = 0.05$, and $\gamma = \frac{1}{12}$. We now choose 60% of the links in the network to have uncertain weights making $\tau \approx 1$. The variance of the uncertainty in the links is chosen small to be able to clearly observe the effects due to a change in neighbors. As we discussed previously, increasing the link uncertainty adds to some numerical inaccuracies in the system causing an additive noise like effect. Furthermore, the additive noise is also assumed to be absent for to facilitate a clear observation of synchronization.

We first choose a network with 6 neighbors per agent. For this network we observe that the system is not able to synchronize and all the agents break up into multiple clusters, with each cluster having a small number of agents, Fig. 5(a). The agents do not obtain enough state information to bind them to the synchronization manifold due to small number of neighbors. We now increase the number of neighbors to 20 for each agent. As the number of neighbors goes up, the agents synchronize to the synchronization manifold extremely well, with very little noise, Fig. 5(b). Furthermore, the rate of synchronization is very high as observed from the simulations, where the agents seem to synchronize within the first 100 seconds and then collectively move to the synchronization manifold. Finally we increase the number of neighbors to 32 for each agent. This increase in the number of neighbors seems to benefit the synchronization initially as all the agents quickly coalesce together. But as they approach the synchronization manifold, the high number of neighbors causes the systems to fluctuate significantly about the manifold, leading to an oscillating band of desynchronized agent states, Fig. 5(c). This is the beginning of a desynchronized states for the agents and any more neighbors for an agent would destabilize the individual system dynamics.

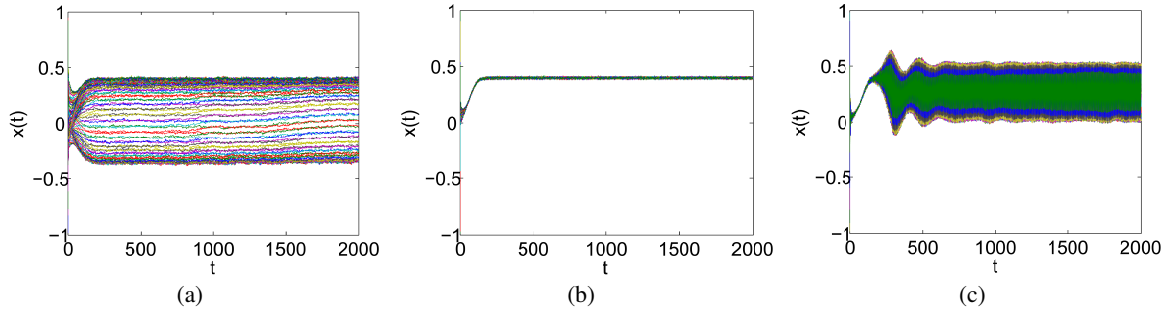


Fig. 5: (a) Time evolution of systems over a 100-node Nearest neighbor network with 6 neighbors per agent, (b) Time evolution of systems over a 100-node Nearest neighbor network with 20 neighbors per agent, (c) Time evolution of systems over a 100-node Nearest neighbor network with 32 neighbors per agent.

V. CONCLUSIONS

We studied the problem of synchronization in complex network systems in the presence of stochastic interaction uncertainty among network nodes. We exploited the identical nature of internal node dynamics to provide a sufficient condition for the network synchronization. The unique feature of the sufficient condition is, it is independent of network size. This makes the sufficient condition attractive from the computational point of view for large-scale network systems. Furthermore, this sufficient condition provides useful insight into the interplay between the internal dynamics of the network nodes, network interconnection topology, location of uncertainty, and uncertainty statistics and their roles in network synchronization. Our results will help understand and compare various complex network topologies for a given internal nodal dynamics.

VI. ACKNOWLEDGMENTS

This work is supported by National Science Foundation ECCS grants 1002053, 1150405, and CNS grant 1329915 (to U.V.).

REFERENCES

- [1] S.H. Strogatz and I. Stewart, *Coupled oscillators and biological synchronization*, Scientific American, 269 (1993), pp. 102–109.
- [2] J.A. Acebrón, L.L. Bonilla, C.J. Pérez Vicente, F. Ritort and R. Spigler, *The kuramoto model: A simple paradigm for synchronization phenomena*, Rev. Mod. Phys., 77 (2005), pp. 137–185.

- [3] T. Danino, O. Mondragon-Palomino, L. Tsimring and J. Hasty, *A synchronized quorum of genetic clocks*, Nature 463 (2010), pp. 326–330.
- [4] F. Dörfler, M. Chertkov and F. Bullo, *Synchronization in complex oscillator networks and smart grids*, Proc. of Nat. Acad. Sci., (2013).
- [5] M. Rohden, A. Sorge, D. Witthaut and M. Timme, *Impact of network topology on synchrony of oscillatory power grids*, Chaos, 24 (2014).
- [6] J. Stout, M. Whiteway, E. Ott, M. Girvan and T. M. Antonsen, *Local synchronization in complex networks of coupled oscillators*, Chaos, 21 (2011).
- [7] P. Erdős and A. Rényi, *On random graphs, I*, Publicationes Mathematicae (Debrecen), 6 (1959), pp. 290–297.
- [8] D. J. Watts and S. H. Strogatz, *Collective dynamics of 'small-world' networks*, Nature, 393 (1998), pp. 409–10.
- [9] L. A. N. Amaral, A. Scala, M. Barthlémy and H. E. Stanley, *Classes of small-world networks*, Proc. of Nat. Acad. Sci., 97 (2000), pp. 11149–11152.
- [10] A. L. Barabási and R. Albert, *Emergence of scaling in random networks*, Science, 286 (1999), pp. 509–512.
- [11] I. Mezic, *On the dynamics of molecular conformation*, Proc. of Nat. Acad. Sci., 103 (2006), pp. 7542–7547.
- [12] E. A. Martens, S. Thutupalli, A. Fourrière and O. Hallatschek, *Chimera states in mechanical oscillator networks*, Proc. of Nat. Acad. Sci., 110 (2013), pp. 10563–10567.
- [13] T. Nishikawa and A. E. Motter, *Network synchronization landscape reveals compensatory structures, quantization, and the positive effect of negative interactions*, Proc. of Nat. Acad. Sci., 107 (2010), pp. 10342–10347.
- [14] X. Wang and G. Chen, *Synchronization in scale-free dynamical networks: Robustness and fragility*, IEEE Trans. on Circuits Syst. I, Fundam. Theory and Appl., 49 (2002), pp. 54–62.
- [15] A. Diwadkar and U. G. Vaidya, *Robust synchronization in nonlinear network with link failure uncertainty*, IEEE Decis. Contr. P., (2010)
- [16] I. Belykh, V. Belykh and M. Hasler, *Blinking models and synchronization in small-world networks with a time-varying coupling*, Physica D, 195 (2004), pp. 188–206.
- [17] M. Hasler, V. Belykh and I. Belykh, *Dynamics of Stochastically Blinking Systems. Part I: Finite Time Properties*, SIAM Journal on Applied Dynamical Systems, 12(2) (2013), pp. 1007–1030.
- [18] M. Hasler, V. Belykh and I. Belykh, *Dynamics of Stochastically Blinking Systems. Part I: Asymptotic Properties*, SIAM Journal on Applied Dynamical Systems, 12(2) (2013), pp. 1031–1084.
- [19] W. Lu, F. M. Atay and J. Jost, *Synchronization of discrete-time dynamical networks with time-varying coupling*, SIAM Journal of Mathematical Analysis, 39(4) (2007), pp. 1231–1259.
- [20] W. Lu, F. M. Atay and J. Jost, *Chaos synchronization in networks of coupled maps with time-varying topologies* European Physics Journal B, 63 (2008), pp. 399–406
- [21] L. C. Garcia del Molino, K. Pakdaman, J. Touboul and G. Wainrib, *Synchronization in random balanced networks*, Phys. Rev. E 88 (2013), pp. 042824.
- [22] S. Sinha and S. Sinha, *Robust emergent activity in dynamical networks*, Phys. Rev. E, 74 (2006), pp. 066117.
- [23] L. Kocarev, U. Parlitz and R. Brown, *Robust synchronization of chaotic systems*, Phys. Rev. E, 61 (2000), pp. 3716–3720.
- [24] Z. Wang, H. Fan and K. Aihara, *Three synaptic components contributing to robust network synchronization*, Phys. Rev. E, 83 (2011), pp. 051905.
- [25] A. Diwadkar and U. G. Vaidya, *Limitation on nonlinear observation over erasure channel*, IEEE Trans. Autom. Control, 58 (2013), pp. 454–459.

- [26] A. Diwadkar and U.G. Vaidya, *Control of LTV systems over uncertain channel*, Int. J. Robust Nonlin., (2012).
- [27] U.G. Vaidya and N. Elia, *Limitation on nonlinear stabilization over packet-drop channels: Scalar case*, Syst. Control Lett., (2012).
- [28] U.G. Vaidya and N. Elia, *Limitation on nonlinear stabilization over erasure channel*, IEEE Decis. Contr. P., (2010), pp. 7551–7556.
- [29] R.Z. Hasminskii, *Stochastic Stability of differential equations*, Sijthoff & Noordhoff, Germantown, MD, (1980).
- [30] Z. Wang, Y. Wang and Y. Liu, *Global synchronization for discrete-time stochastic complex networks with randomly occurred nonlinearities and mixed time delays*, IEEE T. Neural Networ., 21 (2010), pp. 11–25.
- [31] R. Merris, *Laplacian matrices of graphs: a survey*, Linear Algebra Appl., 197/198 (1994), pp. 143 – 176.
- [32] W. Haddad, D. Bernstein, *Explicit construction of quadratic Lyapunov functions for the small gain theorem, positivity, circle and Popov theorems and their application to robust stability. Part II: Discrete-time theory*, Int. J. Robust Nonlin., 4 (1994), pp. 249–265.
- [33] P. Lancaster, L. Rodman, *Algebraic Riccati Equations*, Oxford Science Publications, Oxford, (1995).

APPENDIX

We consider the problem of synchronization in large-scale nonlinear network systems where the scalar dynamics of the individual subsystem is assumed

$$x_{t+1}^k = ax_t^k - \phi(x_t^k) + v_t^k \quad k = 1, \dots, N, \quad (12)$$

where, $x^k \in \mathbb{R}$ are the states of the k^{th} subsystem, and $a > 0$ and $v^k \in \mathbb{R}$ is an independent identically distributed (i.i.d.) additive noise process with zero mean (i.e., $E[v_t^k] = 0$) and variance $E[(v_t^k)^2] = \omega^2$. The function $\phi: \mathbb{R} \rightarrow \mathbb{R}$ is a nonlinear function that satisfies Assumption 1. If the coupling gain is $g > 0$ the individual agent dynamics of the coupled subsystem is given by,

$$x_{t+1}^k = ax_t^k - \phi(x_t^k) + g \sum_{e_{kj} \in E_D} \mu_{kj} (x_t^j - x_t^k) + g \sum_{e_{ki} \in E_U} (\mu_{ki} + \xi_{ki}) (x_t^i - x_t^k) + v_t^k.$$

We denote the deterministic mean graph Laplacian by $\mathcal{L}_M := [\mu_{ij}] \in \mathbb{R}^{N \times N}$ and uncertain graph Laplacian by $\mathcal{L}_R := [\xi_{ij}] \in \mathbb{R}^{N \times N}$. We combine the individual systems to create the network system (\tilde{x}_t) written as,

$$\tilde{x}_{t+1} = (aI_N - g(\mathcal{L}_M + \mathcal{L}_R)) \tilde{x}_t - \tilde{\phi}(\tilde{x}_t) + \tilde{v}_t, \quad (13)$$

where I_N is the $N \times N$ identity matrix, and $\tilde{x}_t = [(x_t^1)' \dots (x_t^N)']'$ and $\tilde{\phi}(\tilde{x}_t) = [(\phi^1)'(x_t^1) \dots (\phi^N)'(x_t^N)]'$.

Since the subsystems are identical, the synchronization manifold is given by $\mathbf{1} = [1, \dots, 1]'$. The dynamics on the synchronization manifold is decoupled from the dynamics off the manifold

and is essentially described by the dynamics of the individual system which could be stable, oscillatory, or complex in nature. We now apply change of coordinates to decompose the system dynamics on and off the synchronization manifold. Let $\mathcal{L}_M = V_M \Lambda_M V_M'$, where V_M is an orthonormal set of vectors given by $V_M = \left[\frac{\mathbf{1}}{\sqrt{N}} \ U_M \right]$, $\mathbf{1} = [1 \ \cdots \ 1]'$ and U_M is an orthonormal set of vectors also orthonormal to $\mathbf{1}$. Let $\tilde{z}_t = V_M' \tilde{x}_t$ and $\tilde{w}_t = V_M' \tilde{v}_t$. Multiplying (13) from the left by $V_M' \otimes I_n$, we obtain

$$\tilde{z}_{t+1} = (aI_N - g(V_M'(\mathcal{L}_M + \mathcal{L}_R)V_M)) \tilde{z}_t - \tilde{\psi}(\tilde{z}_t) + \tilde{w}_t, \quad (14)$$

where $\tilde{\psi}(\tilde{z}_t) = V_M' \tilde{\phi}(\tilde{x}_t)$. We can now write $\tilde{z}_t = \begin{bmatrix} \bar{x}_t & \hat{z}_t \end{bmatrix}'$, $\tilde{\psi}(\tilde{z}_t) := \begin{bmatrix} \bar{\phi}_t & \hat{\psi}_t \end{bmatrix}'$ and $\tilde{w}_t := \begin{bmatrix} \bar{v}_t & \hat{w}_t \end{bmatrix}'$, where

$$\begin{aligned} \bar{x}_t &:= \frac{\mathbf{1}'}{\sqrt{N}} \tilde{x}_t = \frac{1}{\sqrt{N}} \sum_{k=1}^N x_t^k, & \hat{z}_t &:= U_M' \tilde{x}_t \\ \bar{\phi}_t &:= \frac{\mathbf{1}'}{\sqrt{N}} \tilde{\phi}(\tilde{z}_t) = \frac{1}{\sqrt{N}} \sum_{k=1}^N \phi(x_t^k), & \hat{\psi}_t &:= U_M' \tilde{\phi}(\tilde{x}_t). \end{aligned}$$

Furthermore, we have

$$E_{\bar{v}}[\bar{v}_t^2] = \sqrt{N}\omega^2, \quad E_{\bar{v}}[\hat{w}_t \hat{w}_t'] = U_M' E_{\bar{v}}[\tilde{v}_t \tilde{v}_t'] U_M = \omega^2 I_{N-1}.$$

From (14), we obtain

$$\begin{aligned} \bar{x}_{t+1} &= a\bar{x}_t - \bar{\phi}(\bar{x}_t) + \bar{v}_t \\ \hat{z}_{t+1} &= \left(aI_{N-1} - g \left(\hat{\Lambda}_M + U_M' \mathcal{L}_R U_M \right) \right) \hat{z}_t - \hat{\psi}_t + \hat{w}_t, \end{aligned} \quad (15)$$

where $\Lambda_d = \begin{bmatrix} 0 & 0 \\ 0 & \hat{\Lambda}_M \end{bmatrix}$. For the synchronization of system (13), we only need to demonstrate the mean square stability to the origin of \hat{z} dynamics as given in (15). This feature is exploited to derive the sufficiency condition for mean square synchronization of the coupled system as shown in the following lemma.

Lemma 11: Mean square noise to state stability of system described by (15) implies mean square synchronization of the system (13) as given by Definition 1.

Proof: To prove this result, we show the second moment of \hat{z}_t dynamics is equivalent to

the mean square error dynamics for each pair of systems. Then, we apply stability results to the error dynamics to complete the proof. Consider Eq. (15). We have

$$\| \hat{z}_t \|^2 = \hat{z}'_t \hat{z}_t = \tilde{x}'_t (U_d U'_d \otimes I_n) \tilde{x}_t. \quad (16)$$

We have $U_d U'_d = V_d V'_d - \frac{\mathbf{1} \mathbf{1}'}{\sqrt{N} \sqrt{N}} = I_N - \frac{1}{N} \mathbf{1} \mathbf{1}'$. Substituting in (16) we obtain

$$\| \hat{z}_t \|^2 = \frac{1}{2N} \sum_{i=1}^N \sum_{j \neq i, j=1}^N (x_t^i - x_t^j)' (x_t^i - x_t^j). \quad (17)$$

Now, mean square noise to state stability of (15) implies there exists $L > 0$, $K > 0$ and $0 < \beta < 1$, such that

$$\begin{aligned} E_{\Xi} \| \hat{z}_t \|^2 &\leq K \beta^t \| \hat{z}_0 \|^2 + L \omega^2, \\ E_{\Xi} \sum_{k=1}^N \sum_{j \neq k, j=1}^N \| x_t^k - x_t^j \|^2 &\leq K \beta^t \sum_{k=1}^N \sum_{j \neq k, j=1}^N \| x_0^k - x_0^j \|^2 + L \omega^2. \end{aligned}$$

This implies

$$\sum_{k=1}^N \sum_{j \neq k, j=1}^N E_{\Xi} \| x_t^k - x_t^j \|^2 \leq K \beta^t \sum_{k=1}^N \sum_{j \neq k, j=1}^N \| x_0^k - x_0^j \|^2 + L \omega^2. \quad (18)$$

Thus, from (18) we obtain for all systems S_k and S_l ,

$$E_{\Xi} \| x_t^k - x_t^l \|^2 \leq \bar{K}(\tilde{\epsilon}_0) \beta^t \| x_0^k - x_0^l \|^2 + L \omega^2,$$

where $\bar{K}(\tilde{\epsilon}_0) := K \left(1 + \frac{\sum_{i=1, i \neq k}^N \sum_{j=1, j \neq i}^N \| x_0^i - x_0^j \|^2}{\| x_0^k - x_0^l \|^2} \right)$. Hence, the proof. \blacksquare

We will now provide a slightly modified Eq. (15). We know $\mathcal{L}_R = \sum_{e_{ij} \in E_U} \xi_{ij} l_{ij} \hat{l}'_{ij}$, where $l_{ij} \in \mathbb{R}$ has values 1 and -1 in i^{th} and j^{th} entries, respectively, the remaining are zeros. Thus $\hat{l}'_{ij} l_{ij} = 2$ for all $e_{ij} \in E$. Hence, if $\hat{l}_{ij} = U'_M l_{ij}$, we calculate

$$U'_M \mathcal{L}_u U_d = \sum_{e_{ij} \in E_U} \xi_{ij} U'_M l_{ij} \hat{l}'_{ij} U_M = \sum_{e_{ij} \in E_U} \xi_{ij} \hat{l}_{ij} \hat{l}'_{ij},$$

where $\hat{l}'_{ij} \hat{l}_{ij} = 2$. Thus, we can write Eq. (15) as

$$\hat{z}_{t+1} = \left(a I_{N-1} - g \hat{\Lambda}_M - \sum_{e_{ij} \in E_U} \xi_{ij} \hat{l}_{ij} \hat{l}'_{ij} \right) \hat{z}_t - \hat{\psi}(\hat{z}_t) + \hat{w}_t. \quad (19)$$

In Lemma 11 we prove the mean square exponential stability of (19) guarantees the mean square synchronization of the coupled network of Lur'e systems as given by (13). We will now utilize this to provide the sufficiency condition for mean square stabilization of Lur'e systems over a network to prove Theorem 3.

Proof: We first construct an appropriate Lyapunov function, $V(\hat{z}_t) = \hat{z}_t' P \hat{z}_t$, that guarantees mean square stability. We state system (15) is mean square stable, if there exists $P < \delta I_{N-1}$ and

$$P = E_{\Xi} [(A(\Xi)'P - I_{N-1}) (\delta I_{N-1} - P)^{-1} (PA(\Xi) - I_{N-1})] + E_{\Xi} [A(\Xi)'PA(\Xi)] + R_P, \quad (20)$$

where $A(\Xi) = aI_{N-1} - g\hat{\Lambda}_M - gU_d' \mathcal{L}_u U_d$ and $\Xi = \{\xi_{ij}, e_{ij} \in E_U\}$. To show this, consider the expected value of a one-step change in the Lyapunov function, $V(\hat{z}_t)$, as given by

$$\begin{aligned} \Delta V := E_{\Xi_t, v_t} [V(\hat{z}_{t+1}) - V(\hat{z}_t)] &= \psi'(\hat{z}_t) P \psi(\hat{z}_t) + 2\hat{z}_t' E_{\Xi} [A(\Xi)'P] \psi(\hat{z}_t) \\ &+ \hat{z}_t' (E_{\Xi} [A(\Xi)'PA(\Xi)] - P) \hat{z}_t + E_v [\hat{w}_t' P \hat{w}_t]. \end{aligned} \quad (21)$$

Substituting from (20) into (21), and using the algebraic manipulations as adopted in [32] we obtain

$$\Delta V = -\hat{z}_t' R_P \hat{z}_t - E_{\Xi} [\eta_t' \eta_t] - 2\psi'(\hat{z}_t) \left(\hat{z}_t - \frac{\delta}{2} \psi(\hat{z}_t) \right) + \text{trace}(P E_v [\hat{w}_t \hat{w}_t']),$$

where $\eta_t(\Xi(t))$ be given by

$$\eta_t(\Xi(t)) = W^{-\frac{1}{2}} (PA(\Xi) - I_{N-1}) \hat{z}_t - W^{\frac{1}{2}} \psi(\hat{z}_t),$$

where, $W := (\delta I_{N-1} - P)$. From the condition of Assumption 1 and taking $\rho = \text{trace}(P)$, we calculate

$$E_{\Xi_t, v_t} [V(\hat{z}_{t+1}) - V(\hat{z}_t)] < -\hat{z}_t' R_P \hat{z}_t + \rho \omega^2. \quad (22)$$

We know there exists $0 < c_1 < c_2$ such that

$$c_1 \|\hat{z}_t\|^2 \leq V_t \leq c_2 \|\hat{z}_t\|^2 \quad (23)$$

From (22) and (23), and $c_3 = \lambda_{max}(R)$ is the spectral radius of R , we obtain

$$E_{\Xi_t, v_t} [V(\hat{z}_{t+1})] < \left(1 - \frac{c_3}{c_2}\right) V(\hat{z}_t) + \rho\omega^2. \quad (24)$$

Writing $\left(1 - \frac{c_3}{c_2}\right) = \beta$, taking expectation over (Ξ_0^t, v_0^t) and applying (24) recursively we get,

$$E_{\Xi_0^t, v_0^t} [V(\hat{z}_{t+1})] < \beta^t V(\hat{z}_0) + \left(\sum_{i=0}^t \beta^i\right) \rho\omega^2. \quad (25)$$

This gives us $E_{\Xi_0^t, v_0^t} [\|\hat{z}_{t+1}\|^2] < K\beta^t \|\hat{z}_0\|^2 + L\omega^2$, where $K = \frac{c_2}{c_1}$ and $L = \frac{\rho}{(1-\beta)c_1}$. This implies the mean square exponential stability of \hat{z}_t . Also, the equations in (20) can be rewritten using [33] (Proposition 12.1,1) as

$$P = E_{\Xi} [A_0(\Xi)' P A_0(\Xi)] + R_P + \frac{1}{\delta} I_{N-1} + E_{\Xi} [A_0(\Xi)' P (\delta I_{N-1} - P)^{-1} P A_0(\Xi)], \quad (26)$$

where $A_0(\Xi) = a_0 I_{N-1} - g\hat{\Lambda}_M - gU_d' \mathcal{L}_u U_d$ and $a_0 = a - \frac{1}{\delta}$. We observe this condition requires us to find a symmetric Lyapunov function matrix P of order $\frac{N(N-1)}{2}$. We now reduce the order of computation by using network properties. For this, consider $P = pI_{N-1}$ where $p < \delta$ is a positive scalar. This gives us $\delta I_{N-1} > P$. Using this and (19) we rewrite the condition in (26) as follows

$$\begin{aligned} pI_{N-1} &> p(a_0 I_{N-1} - g\hat{\Lambda}_M)'(a_0 I_{N-1} - g\hat{\Lambda}_M) + \frac{p^2}{\delta - p} (a_0 I_{N-1} - g\hat{\Lambda}_M)'(a_0 I_{N-1} - g\hat{\Lambda}_M) + \frac{1}{\delta} I_{N-1} \\ &+ pg^2 \sum_{e_{ij} \in E_U} \sigma_{ij}^2 \hat{\ell}_{ij} \hat{\ell}'_{ij} \hat{\ell}_{ij} \hat{\ell}'_{ij} + \frac{p^2 g^2}{\delta - p} \sum_{e_{ij} \in E_U} \sigma_{ij}^2 \hat{\ell}_{ij} \hat{\ell}'_{ij} \hat{\ell}_{ij} \hat{\ell}'_{ij}. \end{aligned} \quad (27)$$

We know $\hat{\ell}'_{ij} \hat{\ell}_{ij} = \ell'_{ij} U_d U_d' \ell_{ij} = \ell'_{ij} \ell_{ij} = 2$ and

$$\sum_{e_{ij} \in E_U} \sigma_{ij}^2 \hat{\ell}_{ij} \hat{\ell}'_{ij} \hat{\ell}_{ij} \hat{\ell}'_{ij} \leq 2\bar{\gamma} \sum_{e_{ij} \in E_U} \mu_{ij} \hat{\ell}_{ij} \hat{\ell}'_{ij} = 2\bar{\gamma} U_M' \mathcal{L}_U U_M \quad (28)$$

Now suppose there exists τ such that, $\mathcal{L}_U \leq \tau \mathcal{L}_M = \tau (\mathcal{L}_D + \mathcal{L}_U)$. Then we obtain,

$$\tau \geq \frac{\lambda_{N_U}}{\lambda_{N_U} + \lambda_{2_D}} \quad (29)$$

Choosing $\tau = \frac{\lambda_{N_U}}{\lambda_{N_U} + \lambda_{2_D}}$ and using $\mathcal{L}_U \leq \tau \mathcal{L}_M =$ in Eq. (28) we obtain,

$$\sum_{e_{ij} \in E_U} \sigma_{ij}^2 \hat{\ell}_{ij} \hat{\ell}'_{ij} \hat{\ell}_{ij} \hat{\ell}'_{ij} \leq 2\bar{\gamma}\tau U'_M \mathcal{L}_M U_M = 2\bar{\gamma}\tau \hat{\Lambda}_M \quad (30)$$

Now, substituting (28) into (27), a sufficient condition for inequality (27) to hold is given by

$$\begin{aligned} pI_{N-1} &> \left(p + \frac{p^2}{\delta - p} \right) (a_0 I_{N-1} - g \hat{\Lambda}_M)' (a_0 I_{N-1} - g \Lambda_M) \\ &+ \left(p + \frac{p^2}{\delta - p} \right) 2\bar{\gamma}\tau g^2 \hat{\Lambda}_M + \frac{1}{\delta} I_{N-1}. \end{aligned} \quad (31)$$

Equation (31) is essentially a block diagonal equation which provides the sufficient condition for mean square synchronization to be

$$p > \left(p + \frac{p^2}{\delta - p} \right) ((a_0 - g\lambda_j)^2 + 2\bar{\gamma}\tau g^2 \lambda_j) + \frac{1}{\delta} \quad (32)$$

for all eigenvalues λ_j of $\hat{\Lambda}_M$. This is simplified as

$$0 > p^2 + \left((\alpha_0^2 - 1)\delta - \frac{1}{\delta} \right) p + 1, \quad (33)$$

where $\delta > p > 0$ and $\alpha_0^2 = (a_0 - g\lambda)^2 + 2\bar{\gamma}\tau \lambda g^2$ for all $\lambda \in \{\lambda_2, \dots, \lambda_N\}$ are eigenvalues of the deterministic graph Laplacian. Now, for each of these conditions to hold true, we must satisfy condition (33) for the minimum value of α_0^2 with respect to any possible λ . Now, λ^* that provides minimum values for α_0^2 is found by setting $\left. \frac{d\alpha_0^2}{d\lambda} \right|_{\lambda^*} = 0$, giving us $\lambda^* = \frac{a_0}{g} - \bar{\gamma}\tau$. Using λ^* , we know for (33) to be satisfied for all $\lambda \in \{\lambda_2, \dots, \lambda_N\}$, it must satisfy (33) for the farthest such λ from λ^* . Since eigenvalues of a graph Laplacian are positive and monotonic non-decreasing, all we need is to satisfy (33) for λ_{sup} , where

$$\lambda_{sup} = \operatorname{argmax}_{\lambda \in \{\lambda_2, \lambda_N\}} |\lambda - \lambda^*|.$$

This proves the result. ■

We now provide the proof for Lemma 2, which provides a method to design the optimal coupling gain for synchronization.

Proof: The synchronization margin, ρ_{SM} , for a given Laplacian eigenvalue, λ , and coupling

gain, g , is given by the formula

$$\rho_{SM}(\lambda, g) = \frac{1}{2} \left(\kappa(\lambda, g) - \frac{2}{\delta} + \sqrt{\kappa(\lambda, g)^2 - \frac{4}{\delta^2}} \right), \quad (34)$$

where $\kappa(\lambda, g) = 1 + \frac{1}{\delta^2} - (a_0 - \lambda g)^2 - 2\lambda\bar{\gamma}\tau g$, with $a_0 = a - \frac{1}{\delta}$. To maximize the synchronization margin with respect to the coupling gain, g , for a given λ , we must have $\frac{\partial \rho_{SM}(\lambda, g)}{\partial g} = 0$. This gives us

$$\frac{\partial \rho_{SM}(\lambda, g)}{\partial g} = \frac{1}{2} \left(1 + \frac{\kappa(\lambda, g)}{\sqrt{\kappa(\lambda, g)^2 - 4}} \right) \frac{\partial \kappa(\lambda, g)}{\partial g} = 0.$$

Thus, minimizing κ minimizes ρ_{SM} . Therefore, we must have $\frac{\partial \kappa(\lambda, g)}{\partial g} = 0$. This provides us the optimal g for a given λ to be $g^*(\lambda) = \frac{a_0}{\lambda + 2\bar{\gamma}\tau}$ with

$$\kappa(\lambda, g^*(\lambda)) = 1 + \frac{1}{\delta^2} - a_0^2 + \frac{\lambda a_0^2}{\lambda + 2\bar{\gamma}\tau}.$$

To find the synchronization margin at a given g , we need to consider the smallest margin provided by any of the non-zero Laplacian eigenvalues $\{\lambda_2, \dots, \lambda_N\}$. At any instant, the margin provided by any $\lambda \in \{\lambda_2, \dots, \lambda_N\}$ is bounded above by the margin of either λ_2 or λ_N . As the only important eigenvalues for the graph Laplacian which provides limitations to synchronization, are λ_2 and λ_N , we seek the optimal gains for these eigenvalues, which are given by

$$g^*(\lambda_2) = \frac{a_0}{\lambda_2 + 2\bar{\gamma}\tau}, \quad g^*(\lambda_N) = \frac{a_0}{\lambda_N + 2\bar{\gamma}\tau}.$$

Since $\lambda_N \geq \lambda_2$, we have $g^*(\lambda_N) \leq g^*(\lambda_2)$. There also exists a value of gain, g , which provides the exact same synchronization margin for both λ_2 and λ_N . We call this g_e and is obtained by equation $\kappa(\lambda_2, g_e) = \kappa(\lambda_N, g_e)$, which provides

$$2a_0\lambda_2g_e - \lambda_2^2g_e^2 - 2\lambda_2\bar{\gamma}\tau g_e^2 = 2a_0\lambda_Ng_e - \lambda_N^2g_e^2 - 2\lambda_N\bar{\gamma}\tau g_e^2.$$

This gives us for $\lambda_N \neq \lambda_2$ and $\bar{\lambda} = \frac{\lambda_2 + \lambda_N}{2}$,

$$g_e = \frac{a_0}{\bar{\lambda} + \bar{\gamma}\tau}.$$

Furthermore, the κ value for g_e is given by

$$\kappa(\lambda_N, g_e) = 1 + \frac{1}{\delta^2} - a_0^2 + \frac{4\lambda_2\lambda_N a_0^2}{(\lambda_N + \lambda_2 + 2\bar{\gamma}\tau)^2}.$$

Now, since $\lambda_N \geq \lambda_2$, we have $\lambda_2 - \lambda_N \leq 0 \leq 2\bar{\gamma}\tau$. This gives us $\lambda_N + \lambda_2 + 2\bar{\gamma}\tau \leq 2(\lambda_N + 2\bar{\gamma})\tau$ and $g^*(\lambda_N) \leq g_e$. Now, we also have $g_e \leq g^*(\lambda_2)$ iff $2\bar{\gamma} < \lambda_N - \lambda_2$ and $g^*(\lambda_2) \leq g_e$ iff $\lambda_N - \lambda_2 \leq 2\bar{\gamma}\tau$. It is easy to see $g_e < g^*(\lambda_2)$, margin at $g^*(\lambda_2)$ is dictated by $\rho_{SM}(\lambda_N, g^*(\lambda_2)) < \rho_{SM}(\lambda_2, g^*(\lambda_2))$. As $\rho_{SM}(\lambda_N, g^*(\lambda_2)) < \rho_{SM}(\lambda_N, g_e)$, it makes the optimal gain as g_e . In the case for $g^*(\lambda_2) < g_e$, margin at $g^*(\lambda_2)$ is dictated by $\rho_{SM}(\lambda_2, g^*(\lambda_2)) < \rho_{SM}(\lambda_N, g^*(\lambda_2))$. Since $\rho_{SM}(\lambda_2, g^*(\lambda_2)) < \rho_{SM}(g_e)$, it makes the optimal gain as $g^*(\lambda_2)$. Hence defining, $\chi := \max\{\lambda_N, \lambda_2 + 2\bar{\gamma}\tau\}$, we can write the optimal gain as

$$g^* = \frac{2a_0}{\chi + \lambda_2 + 2\bar{\gamma}\tau},$$

and with, $\nu := 1 + \frac{1}{\delta^2} - a_0^2$, the optimal synchronization margin is given by

$$\rho_{SM}(\lambda_2, g^*) = \frac{1}{2} \left(\nu - \frac{2}{\delta} + \chi\lambda_2(g^*)^2 + \sqrt{(\nu + \chi\lambda_2(g^*)^2) - \frac{4}{\delta^2}} \right).$$

■

For $G(V, E)$ with node set V and edge set E , let E_V be all possible connections between nodes in V . Then, for $\tilde{E} = E_V \setminus E$ the graph $\tilde{G} = (V, \tilde{E})$ be the compliment of G . Let $0 = \lambda_1 < \lambda_2 \leq \dots \leq \lambda_N$ be the eigenvalues of G and $0 = \tilde{\lambda}_1 < \tilde{\lambda}_2 \leq \dots \leq \tilde{\lambda}_N$ be the eigenvalues of \tilde{G} . We now state a lemma connecting the eigenvalues of graph G and its complement \tilde{G} , [31].

Lemma 12: Let $G \equiv (V, E)$ be a graph on $|V| = N$ nodes. Suppose $\tilde{G} \equiv (V, \tilde{E})$ is the complement of G , such that $\tilde{G} = K_N \setminus G$, where K_N is the complete graph on N vertices. Let \mathcal{L}_G and $\mathcal{L}_{\tilde{G}}$ be the Laplacian matrices of G and \tilde{G} with eigenvalues, $0 = \lambda_1 \leq \lambda_2 \leq \dots \leq \lambda_N$ and $0 = \tilde{\lambda}_1 \leq \tilde{\lambda}_2 \leq \dots \leq \tilde{\lambda}_N$, respectively. Then, we must have

$$\tilde{\lambda}_1 = \lambda_1 = 0, \tilde{\lambda}_i = N - \lambda_{N-i+2}, \forall i \in \{2, \dots, N\}. \quad (35)$$